Highly efficient electron transport layer with weak pinning and low barrier contact for solar cells: monolayer GaN on 2D lead-free perovskite

Pengjie Fu,[a] Xunhua Zhao,[*,a]

Table S1. The band gaps of $CsPbI_3$ and GaN calculated using different methods. For the comparison, previous reports on the band gaps of $CsPbI_3$ and GaN were also listed.

E_g(eV)	PBE	SOC	HSE+SOC	Meta-GGA	Previous works
$CsPbI_3$	1.316	1.503	1.647	1.732	1.67[1],1.73[2]
GaN	1.523	1.691	3.359	3.491	3.39[3],3.47[4]

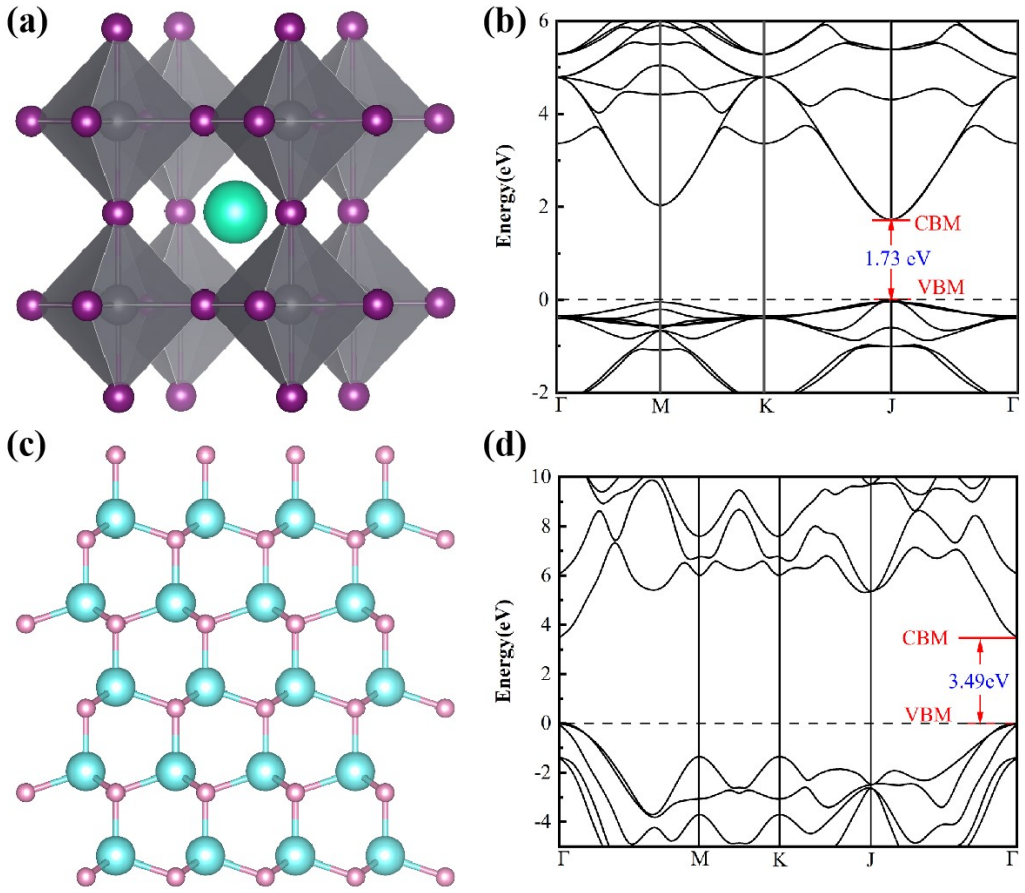

Figure S1. Structures diagram of (a) bulk $Cs_4Pb_3I_{12}$ and (c) bulk GaN. Band structures of (b) bulk $Cs_4Pb_3I_{12}$ and (d) bulk GaN. The zero of the Fermi energy is set at VBM.

The above results indicate that the calculation method we used is approximately equal to the experimental values, so the same method will be used in subsequent system studies.

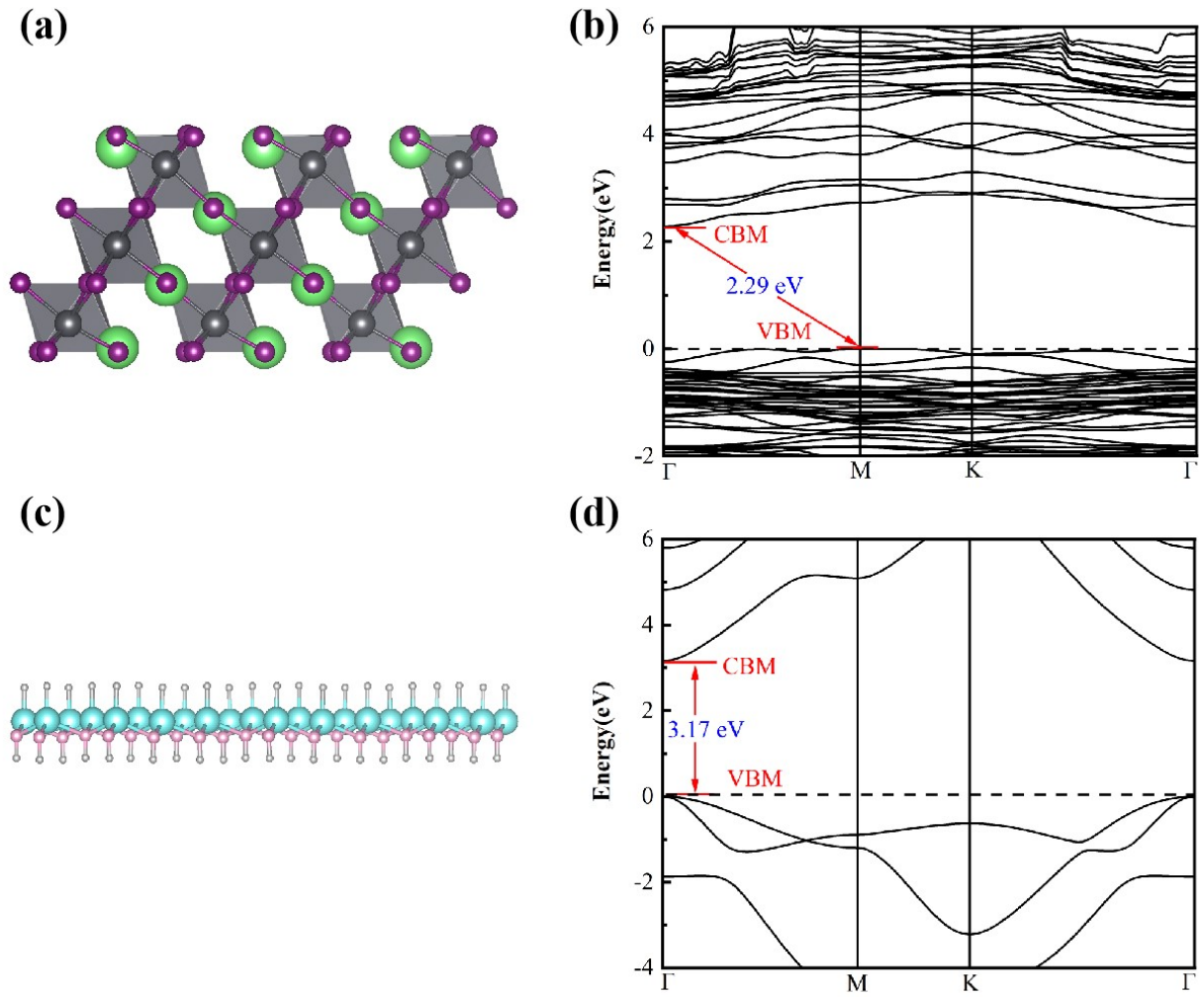

Figure S2. Structures diagram of (a) 2D $Cs_4Pb_3I_{12}$ and (c) 2D GaN. Band structures of (b) 2D $Cs_4Pb_3I_{12}$ and (d) 2D GaN. The zero of the Fermi energy is set at VBM.

Table S2. Surface energies (γ_s) of $Cs_3[M]Pb_3I_{12}$ (M= Ba, Sn, Sr, Mg, Ca, Zn, Cu) nanosheets.

	Ba	Sn	Sr	Mg	Ca	Zn	Cu
$\gamma_{s(meV/Å^2)}$	−32.46	−19.54	−12.55	35.13	28.79	38.14	40.21

$$\gamma_s = \frac{E_{total} - n_v E_{CsPbI_3} + \sum \Delta n_M \mu_M}{2A} \quad \text{(S1)}$$

where E_{total} and E_{CsPbI_3} are total energies of 2D $Cs_3MPb_3I_{12}$ nanosheets and $CsPbI_3$ in cubic bulk, respectively. A is the surface area of nanosheets, n_v is the number of $CsPbI_3$ formula unit in 2D nanosheets, μ_M is the chemical potential of atomic species M (M = Ba, Sn, Sr, Mg, Ca, Zn, Cu), and Δn_M is the difference of atom numbers between the given 2D structure and n_v bulk $CsPbI_3$.

Table S3. Quantification of interface gap states by integrated DOS within the band-gap window.

	$Cs_3YPb_3I_{12}$/GaN	$Cs_3YSr_3I_{12}$/GaN
I_{gap}(states/cell)	0.017	0.45

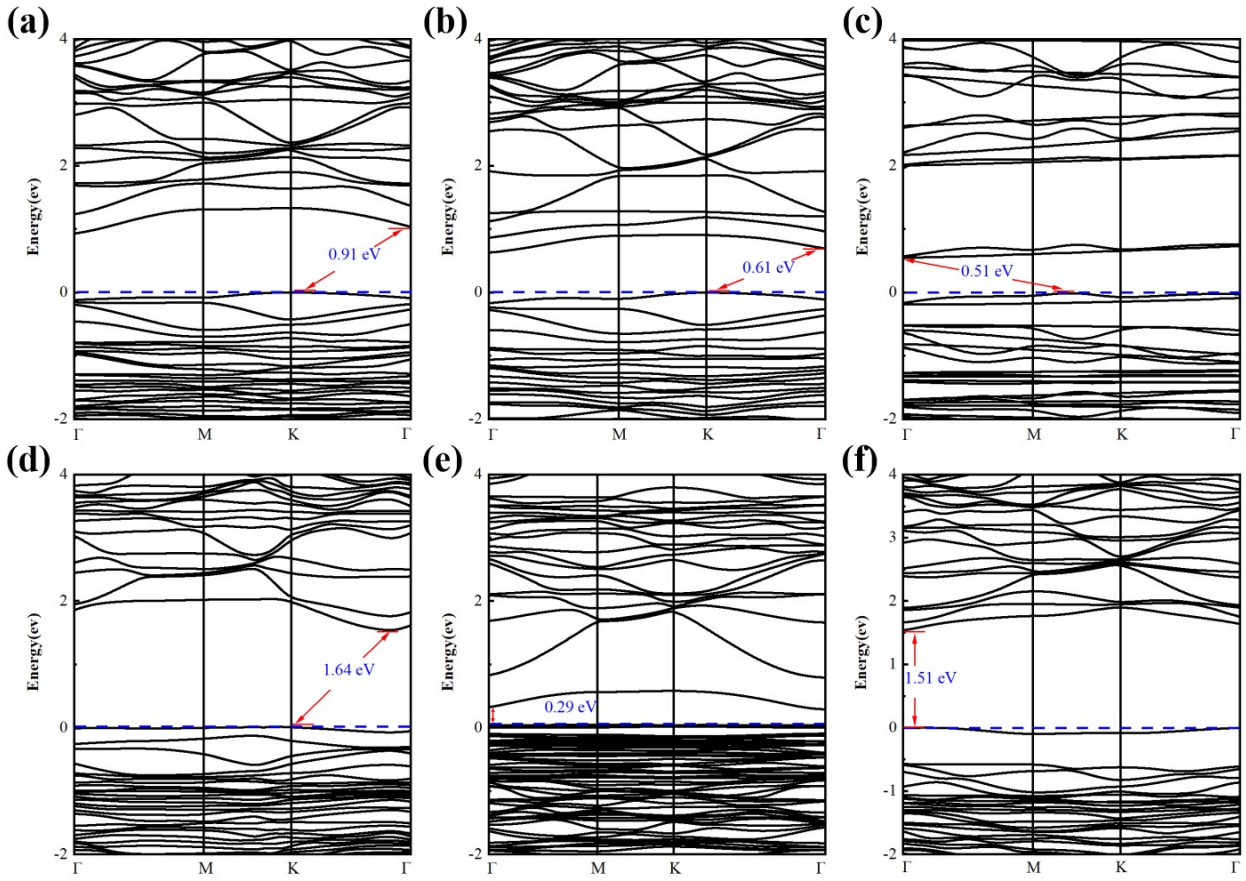

Figure S3. Band structures of $Cs_3[M_2]Pb_3I_{12}$ (M_2=Al, Ln, Tl, La, Bi, Ga) passivated with different metallic elements (a) Al, (b) Ln, (c) Tl, (d) La, (e) Bi, and (f) Ga, respectively.

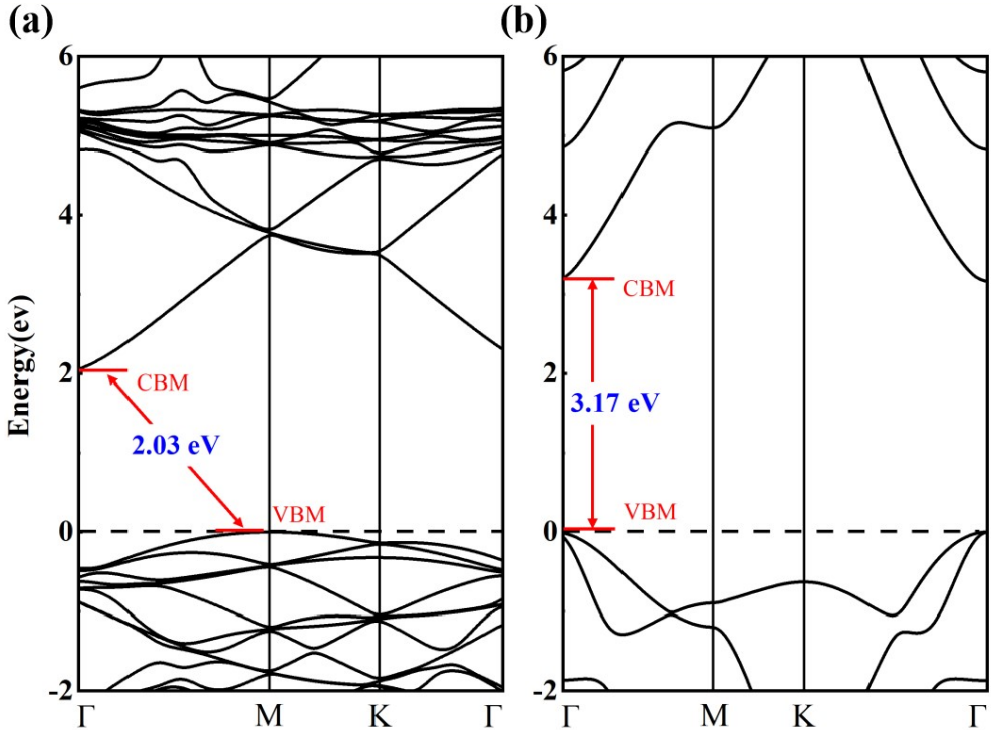

Figure S4. Band structures of (a) un-passivated 2D GaN and (b) passivated 2D GaN, respectively.

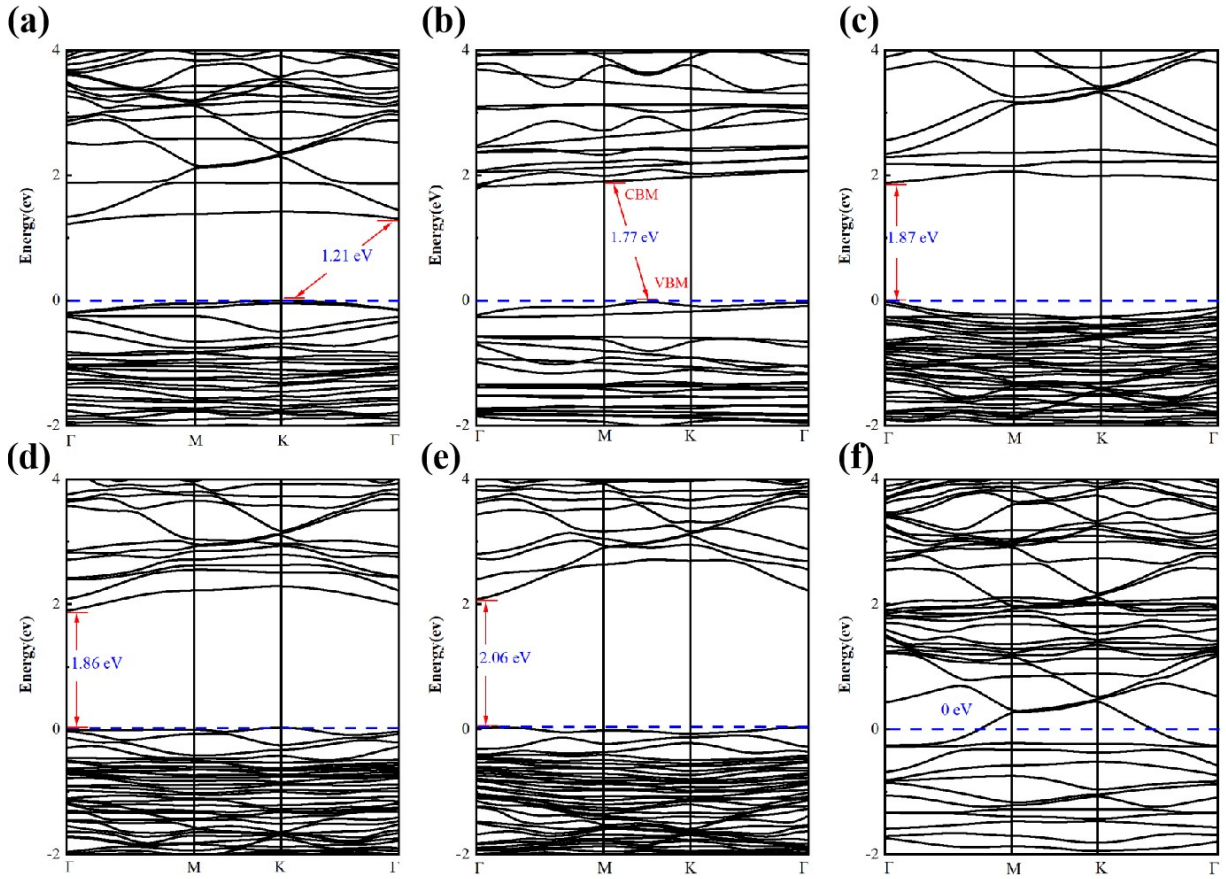

Figure S5. Band structures of $Cs_3Y[M_3]_3I_{12}$/GaN structure (M_3=Ba, Ca, Mg, Sn, Zn, Sr) passivated with different metallic elements (a) Ba, (b) Ca, (c) Mg, (d) Sn, (e) Zn, and (f) Sr, respectively. The zero of the Fermi energy is set at VBM.

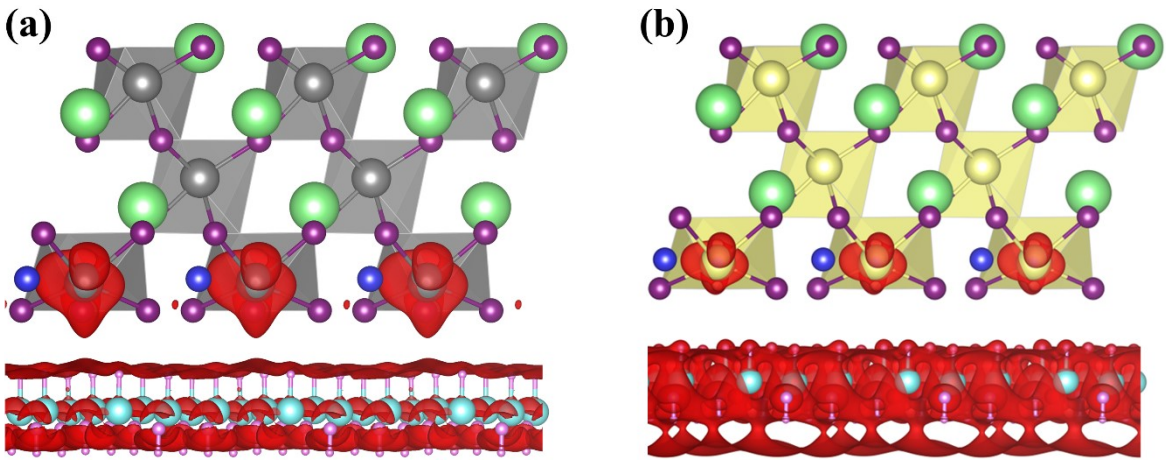

Figure S6. Charge-density distributions of band-edge states of (a) $Cs_3YPb_3I_{12}$/GaN and (b) $Cs_3YSr_3I_{12}$/GaN

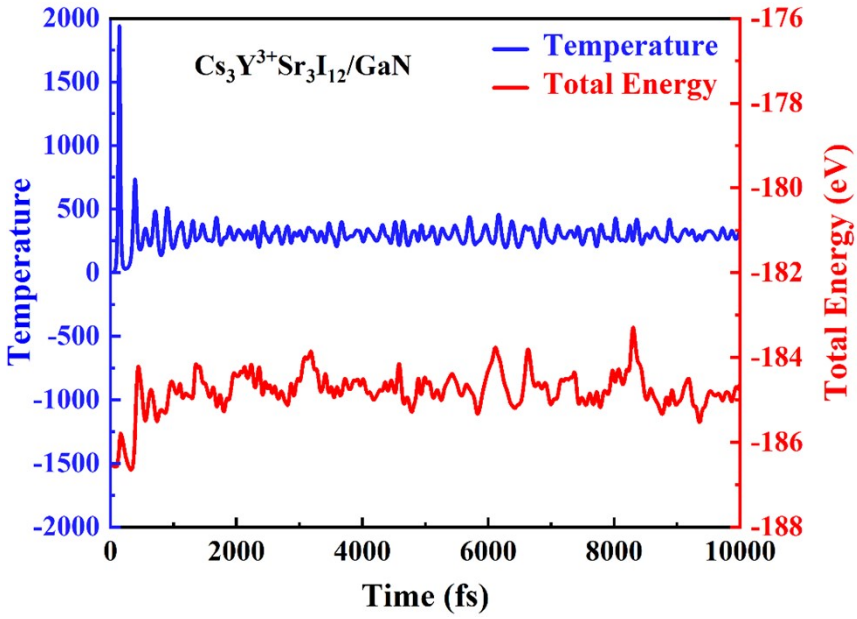

Figure S7. Temperature and total energy profiles from AIMD simulations of the $Cs_3Y^{3+}Sr_3I_{12}$/GaN interface (2 fs timestep, 10 ps).

Table S4. Elastic stiffness constants C_{ij} and stability of $Cs_3YSr_3I_{12}$/GaN heterostructures with different interfacial configurations.

Ga-top	**C_{11}**	**C_{12}**	**C_{13}**	**C_{14}**	**C_{15}**	**C_{16}**	**C_{21}**	**C_{22}**	**C_{23}**	**C_{24}**	**C_{25}**	**C_{26}**	**stable**
	123.04	81.67	-1.66	-6.33	9.84	-7.63	52.86	63.07	10.54	10.33	-22.78	14.92	
	C_{31}	**C_{32}**	**C_{33}**	**C_{34}**	**C_{35}**	**C_{36}**	**C_{41}**	**C_{42}**	**C_{43}**	**C_{44}**	**C_{45}**	**C_{46}**	
	-1.64	10.51	-8.74	-6.59	-2.12	15.14	-6.34	10.33	-6.57	59.54	-9.05	4.28	
	C_{51}	**C_{52}**	**C_{53}**	**C_{54}**	**C_{55}**	**C_{56}**	**C_{61}**	**C_{62}**	**C_{63}**	**C_{64}**	**C_{65}**	**C_{66}**	
	-9.84	-22.78	-2.13	9.15	5.93	-1.61	-7.63	14.91	15.17	4.29	-1.61	16.89	
N-top	**C11**	**C12**	**C13**	**C14**	**C15**	**C16**	**C21**	**C22**	**C23**	**C24**	**C25**	**C26**	**unstable**
	63.07	57.86	14.95	18.64	9.57	8.22	73.94	7.78	6.58	-2.36	1.21	-2.21	
	C31	**C32**	**C33**	**C34**	**C35**	**C36**	**C41**	**C42**	**C43**	**C44**	**C45**	**C46**	
	14.95	8.58	11.49	14.27	5.57	16.12	18.64	-2.48	11.27	10.34	3.59	2.42	
	C51	**C52**	**C53**	**C54**	**C55**	**C56**	**C61**	**C62**	**C63**	**C64**	**C65**	**C66**	
	8.56	2.25	5.56	3.59	6.81	23.53	9.22	-2.51	16.11	3.42	23.53	5.37	

Taking $Cs_3YSr_3I_{12}$/GaN heterostructures as an example, both configurations have the triclinic symmetry, resulting in thirty-six independent elastic constants as follows[5]:

$$C = \begin{pmatrix} C_{11} & C_{12} & C_{13} & C_{14} & C_{15} & C_{16} \\ C_{21} & C_{22} & C_{23} & C_{24} & C_{25} & C_{26} \\ C_{31} & C_{32} & C_{33} & C_{34} & C_{35} & C_{36} \\ C_{41} & C_{42} & C_{43} & C_{44} & C_{45} & C_{46} \\ C_{51} & C_{52} & C_{53} & C_{54} & C_{55} & C_{56} \\ C_{61} & C_{62} & C_{63} & C_{64} & C_{65} & C_{66} \end{pmatrix} \quad \text{(S2)}$$

$$\begin{cases} First-order: C_{11} > 0 \\ Second-order: C_{11}C_{12} - C_{12}^2 > 0 \\ Third-order: C_{11}C_{22}C_{33} + 2C_{12}C_{13}C_{23} - C_{11}C_{23}^2 - C_{22}C_{13}^2 - C_{33}C_{12}^2 > 0 \\ Fourth-order: C_{11}\left(C_{22}C_{33}C_{44} + 2C_{23}C_{24}C_{34} - C_{33}C_{24}^2 - C_{22}C_{34}^2 - C_{44}C_{23}^2\right) - C_{12}\left(C_{12}C_{33}C_{44} + C_{23}C_{14}C_{34} + C_{13}C_{24}C_{34} - C_{33}C_{14}C_{24} - C_{12}C_{34}^2 - C_{13}C_{23}C_{44}\right) + C_{13}\left(C_{12}C_{23}C_{44} + C_{22}C_{14}C_{34} + C_{13}C_{24}^2 - C_{23}C_{14}C_{24} - C_{12}C_{24}C_{34} - C_{22}C_{13}C_{44}\right) - C_{14}\left(C_{12}C_{23}C_{34} + C_{22}C_{33}C_{14} + C_{13}C_{23}C_{24} - C_{14}C_{23}^2 - C_{12}C_{33}C_{24} - C_{22}C_{13}C_{34}\right) > 0 \\ Fifth-order: C_{11}(a-b+c-d) - C_{12}(e-f+g-h) + C_{13}(i-j+k-l) - C_{14}(m-n+o-p) + C_{15}(q-r+s-t) > 0 \\ Sixth-order: \sum_{i=1}^{20} A_i B_i > 0 \end{cases}$$

Among:

a = $C_{22}(C_{33}C_{44}C_{55} + 2C_{34}C_{35}C_{45} - C_{44}C^2_{35} - C_{33}C^2_{45} - C_{55}C^2_{34})$

b = $C_{23}(C_{23}C_{44}C_{55} + C_{34}C_{25}C_{45} + C_{24}C_{35}C_{45} - C_{44}C_{25}C_{35} - C_{23}C^2_{45} - C_{24}C_{34}C_{55})$

c = $C_{24}(C_{23}C_{34}C_{55} + C_{33}C_{45}C_{25} + C_{24}C^2_{35} - C_{34}C_{25}C_{35} - C_{23}C_{35}C_{45} - C_{33}C_{24}C_{55})$

d = $C_{25}(C_{23}C_{34}C_{45} + C_{33}C_{44}C_{25} + C_{24}C_{34}C_{35} - C^2_{34}C_{25} - C_{23}C_{44}C_{35} - C_{33}C_{24}C_{45})$

e = $C_{12}(C_{33}C_{44}C_{55} + 2C_{34}C_{35}C_{45} - C_{44}C^2_{35} - C_{33}C^2_{45} - C_{55}C^2_{34})$

f = $C_{23}(C_{13}C_{44}C_{55} + C_{34}C_{15}C_{45} + C_{14}C_{35}C_{45} - C_{44}C_{15}C_{35} - C_{13}C^2_{45} - C_{14}C_{34}C_{55})$

g = $C_{24}(C_{13}C_{34}C_{55} + C_{33}C_{45}C_{15} + C_{14}C^2_{35} - C_{34}C_{15}C_{35} - C_{13}C_{35}C_{45} - C_{33}C_{14}C_{55})$

h = $C_{25}(C_{13}C_{34}C_{45} + C_{33}C_{44}C_{15} + C_{14}C_{34}C_{35} - C^2_{34}C_{15} - C_{13}C_{44}C_{35} - C_{33}C_{14}C_{45})$

i = $C_{12}(C_{23}C_{44}C_{55} + C_{34}C_{25}C_{45} + C_{24}C_{35}C_{45} - C_{44}C_{25}C_{35} - C_{23}C^2_{45} - C_{24}C_{34}C_{55})$

j = $C_{22}(C_{13}C_{44}C_{55} + C_{34}C_{15}C_{45} + C_{14}C_{35}C_{45} - C_{44}C_{15}C_{35} - C_{13}C^2_{45} - C_{14}C_{34}C_{55})$

k = $C_{24}(C_{13}C_{24}C_{55} + C_{23}C_{15}C_{45} + C_{14}C_{25}C_{35} - C_{24}C_{15}C_{35} - C_{13}C_{25}C_{45} - C_{23}C_{14}C_{55})$

l = $C_{25}(C_{13}C_{24}C_{45} + C_{23}C_{44}C_{15} + C_{14}C_{34}C_{25} - C_{24}C_{34}C_{15} - C_{13}C_{44}C_{25} - C_{23}C_{14}C_{45})$

m = $C_{12}(C_{23}C_{34}C_{55} + C_{33}C_{25}C_{45} + C_{24}C^2_{35} - C_{34}C_{25}C_{35} - C_{23}C_{35}C_{45} - C_{33}C_{24}C_{55})$

n = $C_{22}(C_{13}C_{34}C_{55} + C_{33}C_{15}C_{45} + C_{14}C^2_{35} - C_{34}C_{15}C_{35} - C_{13}C_{35}C_{45} - C_{33}C_{14}C_{55})$

o = $C_{23}(C_{13}C_{24}C_{55} + C_{23}C_{45}C_{15} + C_{14}C_{25}C_{35} - C_{24}C_{15}C_{35} - C_{13}C_{25}C_{45} - C_{23}C_{14}C_{55})$

$p = C_{25}(C_{13}C_{24}C_{35} + C_{23}C_{34}C_{15} + C_{33}C_{14}C_{25} - C_{33}C_{24}C_{15} - C_{13}C_{34}C_{25} - C_{23}C_{14}C_{35})$

$q = C_{12}(C_{23}C_{34}C_{45} + C_{33}C_{44}C_{25} + C_{24}C_{34}C_{35} - C_{25}C^2_{34} - C_{23}C_{44}C_{35} - C_{24}C_{33}C_{45})$

$r = C_{22}(C_{13}C_{34}C_{45} + C_{33}C_{44}C_{15} + C_{14}C_{34}C_{35} - C_{15}C^2_{34} - C_{13}C_{44}C_{35} - C_{33}C_{14}C_{45})$

$s = C_{23}(C_{13}C_{24}C_{45} + C_{23}C_{44}C_{15} + C_{14}C_{25}C_{34} - C_{34}C_{24}C_{15} - C_{13}C_{25}C_{44} - C_{14}C_{23}C_{45})$

$t = C_{24}(C_{13}C_{24}C_{35} + C_{23}C_{34}C_{15} + C_{14}C_{25}C_{33} - C_{33}C_{24}C_{15} - C_{13}C_{34}C_{25} - C_{23}C_{14}C_{35})$

The calculated elastic constants of $Cs_3YSr_3I_{12}$/GaN (0001) heterojunction are shown in Table S2. According to the comparison method of different crystal systems, it is determined to be a triclinic symmetric crystal system. Therefore, the judgment method is as shown above. Based on the mechanical stability criterion, we found that only the $Cs_3YSr_3I_{12}$/GaN heterojunction with Ga-top configuration has high stability, while the N-top configuration is unstable.

Table S5. Electron affinity (χ) of $Cs_3[M_2]Sr_3I_{12}$ (M_2= Sc, Al, Y, Ln, Tl, La, Bi, Ga) nanosheets.

	Sc	Al	Y	Ln	Tl	La	Bi	Ga
χ (eV)	2.36	1.65	−2.47	2.01	3.48	2.52	1.51	1.89

Usually, energy bands will bend near the surface due to the presence of surface states. The energy difference from the minimum value of the conduction band to the vacuum energy level E_0 at the surface is the electron affinity. The difference between E_0 and E_f is the material's work function. In order for electrons in the conduction band to escape into the vacuum, sufficient energy needs to be given to overcome the positive potential barrier on the surface. Generally speaking, the value of electron affinity chi is between 3 eV and 4 eV. Positron Affinity (PEA) surface refers to the surface where the vacuum energy level is located above the lowest point of the bulk conduction band. By special treatment of certain semiconductor surfaces, the vacuum level can be reduced to below the minimum value of the bulk conduction band. In this case, due to the fact that the surface bending band region of NEA materials is usually only a few hundred angstroms wide, it will not have a significant impact on the excitation and electron transport processes inside the material. The term 'negative electron affinity' more accurately describes the effective electron affinity being negative.

The above results show that only Y doped $Cs_3YSr_3I_{12}$/GaN (0001) heterojunction have negative electron affinity, while the rest of the doped $Cs_3[M_2]Sr_3I_{12}$ (M_2= Sc, Al, Ln, Tl, La, Bi, Ga) heterojunctions have positive electron affinity.

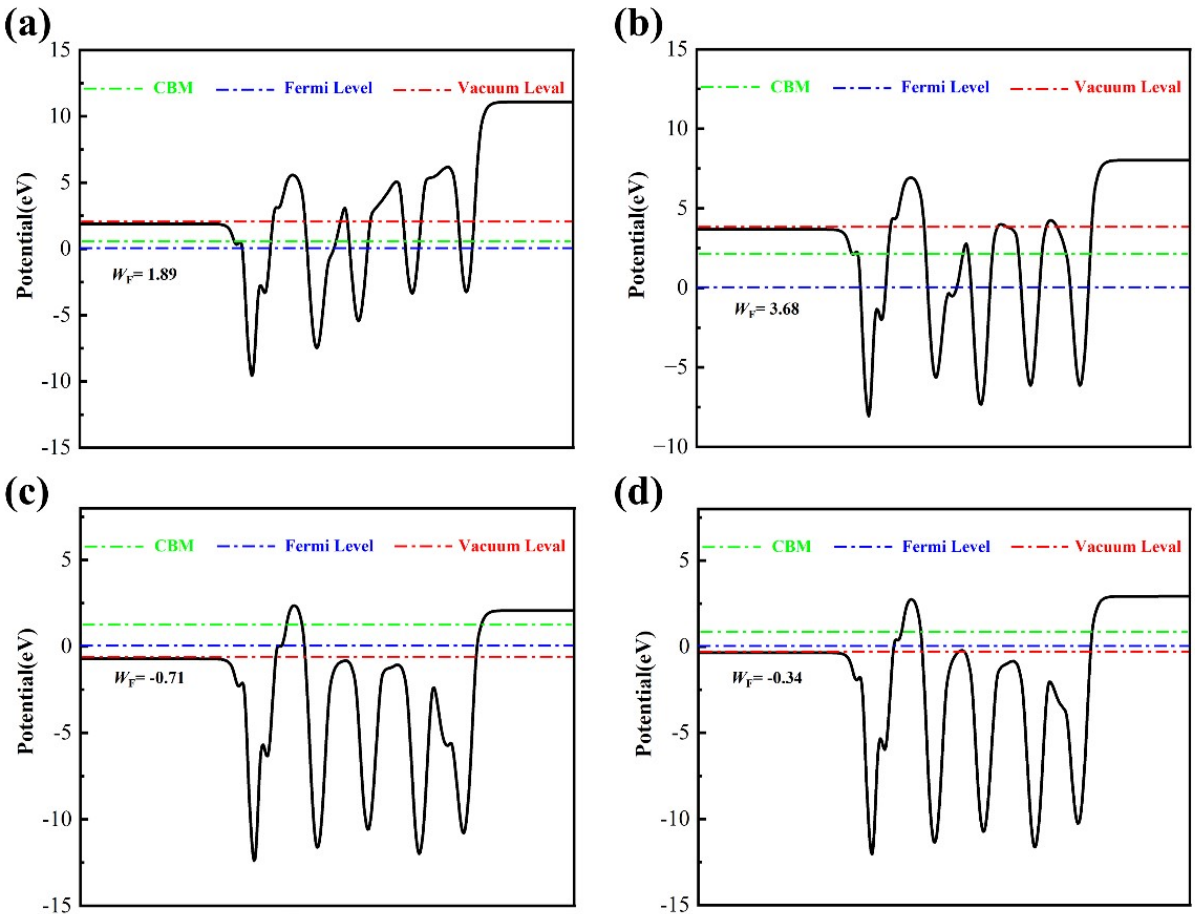

Figure S8. Electrostatic potential distributions of (a) I-termination/Ga-top, (b) I-termination/N-top, (c) Cs-termination/Ga-top, (d) Cs-termination/N-top.

Table S6. Electron affinity (χ) of $Cs_3YSr_3I_{12}$/GaN structure with different termination planes.

	I-termination/Ga-top	I-termination/N-top	Cs-termination/Ga-top	Cs-termination/N-top
χ (eV)	0.96	2.44	−1.58	−1.12

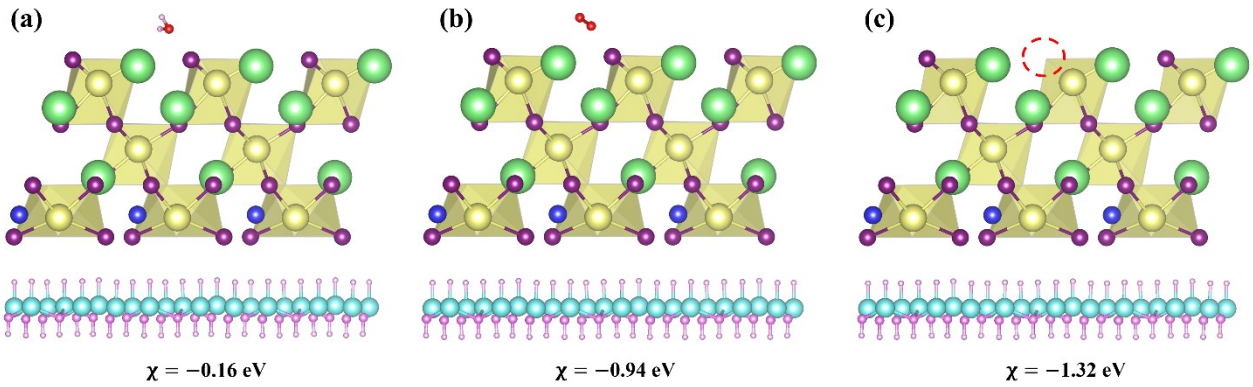

Figure S9. The structural diagrams and the negative electron affinity χ of (a) H_2O, (b) O_2 and (c) I vacancy defects adsorption.

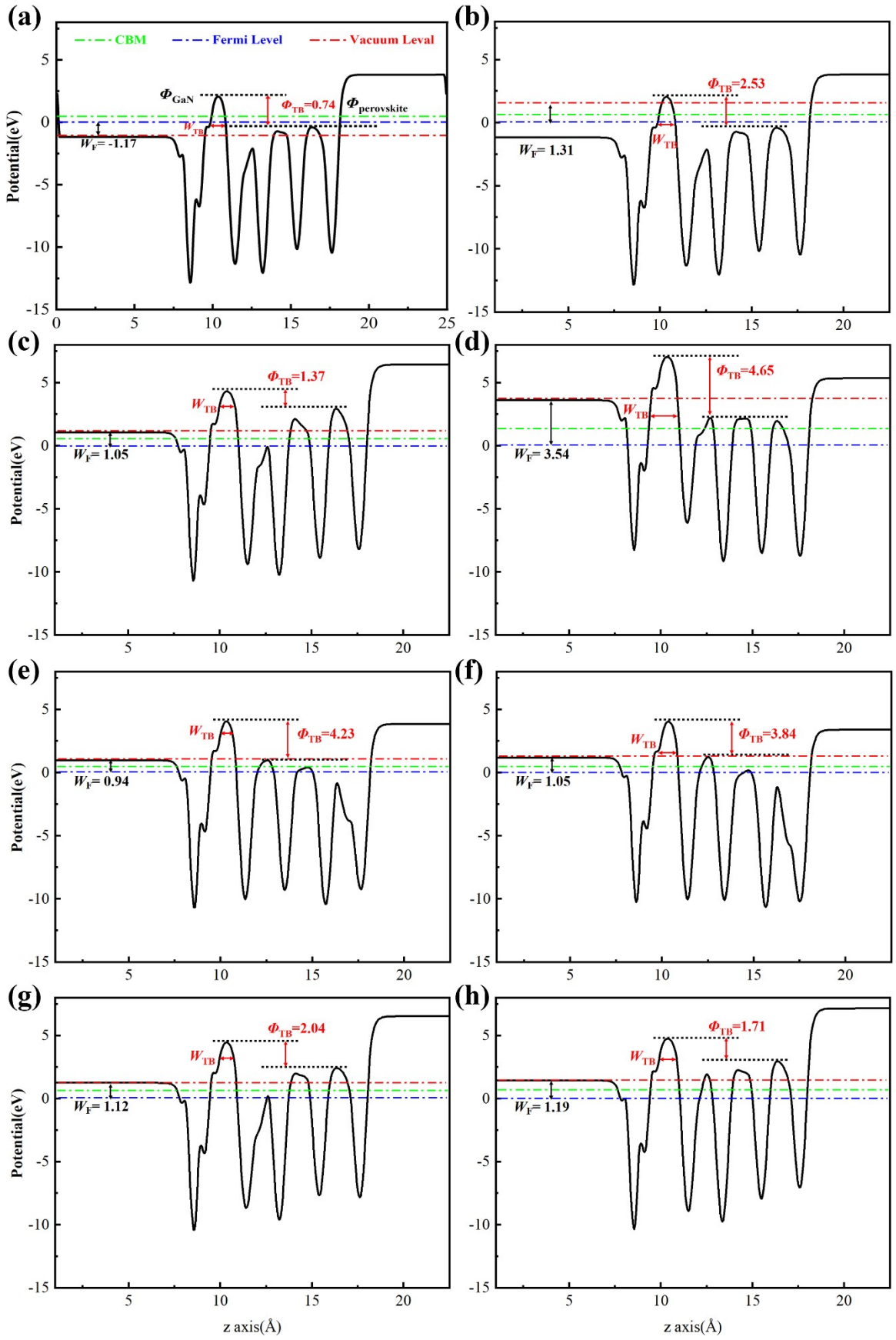

Figure S10. Electrostatic potential distributions of 2D $Cs_3[M_2]Sr_3I_{12}$ (M_2= Y, Sc, Al, Ln, Tl, La, Bi, Ga) heterostructures. Electrostatic potentials and tunnelling barrier of (a) Y, (b) Sc, (c) Al, (d) Ln, (e) Tl, (f) La, (g) Bi, and (h) Ga.

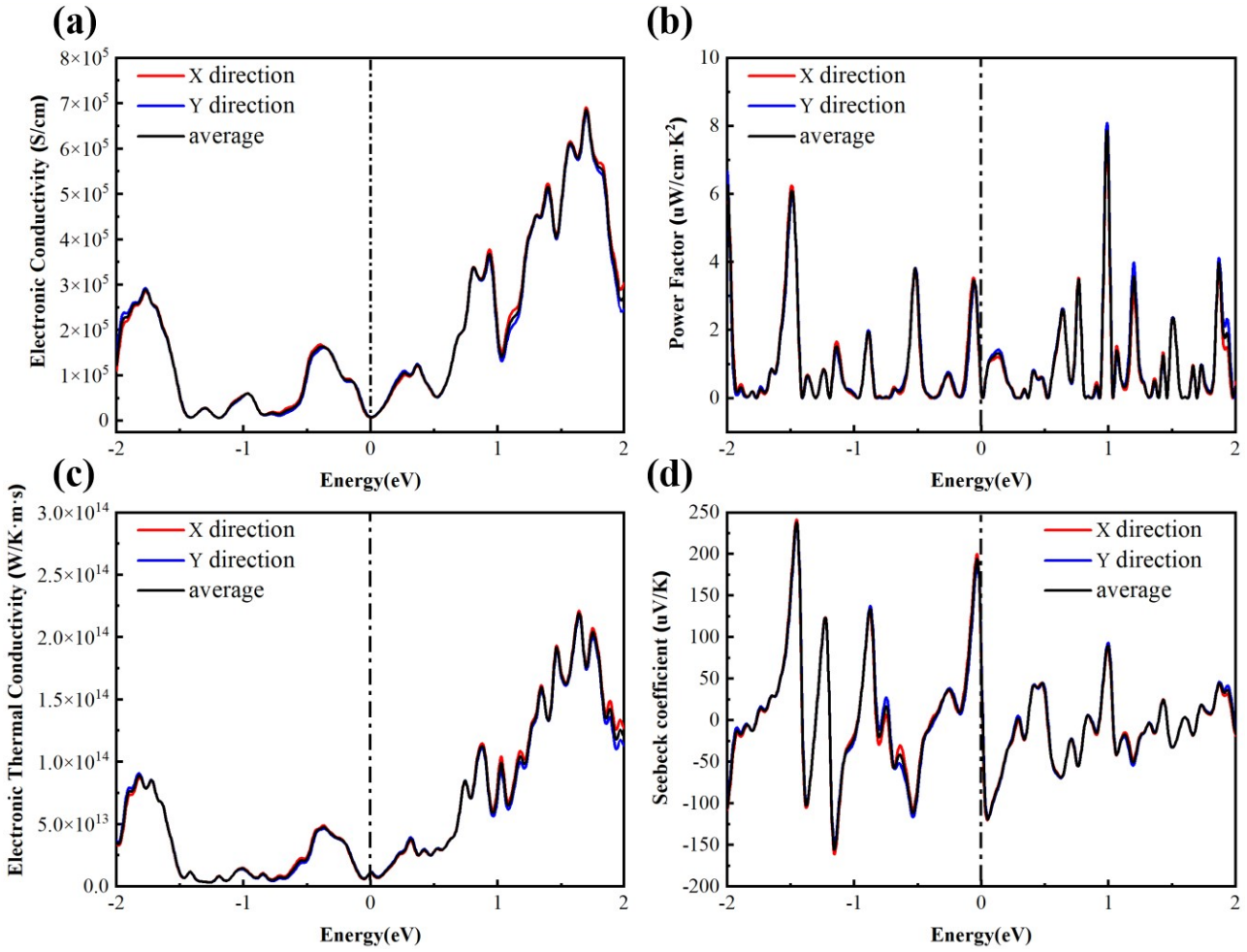

Figure S11. (a) Electronic conductivity, (b) Power factor, (c) Electronic thermal conductivity and (d) Seebeck coefficient of $Cs_3YSr_3I_{12}$/GaN DSH.

The relaxation time τ is required to calculate the electrical conductivity. By utilizing the deformation potential (DP) theory, in combined with the effective mass approximation, the τ can be calculated as[6]

$$\tau = \frac{um^*}{e} = \frac{2\hbar^3 C}{3k_B T m^* E} \quad \text{(S3)}$$

$$C = \left[\partial^2 E / \partial (\Delta a/a_0)^2\right]/S_0 \quad \text{(S4)}$$

where C is the elastic constant, e is the deformation potential energy, m^* is the effective mass, u is the mobility of carriers, including electrons and holes, $\hbar$ is the reduced Planck constant, T is the temperature, E is the total energy of the system. Δa is the change of the lattice constant, $\Delta a/a_0$ is the magnitude of the uniaxial stress, and S_0 is the bottom area of the two-dimensional material.

We use VASPKIT to process the calculated data. The implementation algorithm can be found in the literature (Computer Physics Communications 175 (2006) 67-71).

Step 1: prepare the input file for VASP (INCAR).

ISPIN= 1

LREAL = FALSE. (Projection operators: automatic)

LWAVE = TRUE. (Write WAVECAR or not)

LCHARG = TRUE. (Write CHGCAR or not)

ADDGRID= TRUE. (Increase grid, helps GGA convergence)

Static Calculation

ISMEAR = 0 (gaussian smearing method)

SIGMA = 0.05 (please check the width of the smearing)

LORBIT = 11 (PAW radii for projected DOS)

NEDOS =2001 (DOSCAR points)

NELM =60 (Max electronic SCF steps)

EDIFF =1E-08 (SCF energy convergence, in eV)

Step 2: Use VASPKIT 681 function to output K-point file for transport property calculation.

Step 3: Perform VASP calculation.

Step 4: Prepare INPUT.in file for calculation as follow：

1 (1 for gradient method with constant relaxation time approximation）

2D (2D for slab, 3D for bulk）

-2.0 2.0 (Minimum and maximum values of chemical potential with respect to Fermi energy）

1000 (Number of intervals between the minimum and maximum chemical potential values)

300.0 (Temperature (float type, in units of K))

1.0 (Relaxation time (float type, in units of s), Set 1.0 if you don't know the exact relaxation time)

0.0 (Desired gap value in scissor correction (float type, in units of V), Zero means make no correction, available only non-spin-polarization calculation)

1 (Finite difference method (integer type))

After the completion of VASP operation, use the VASPKIT 682 function to calculate the transport properties. Ending the calculation will generate files such as conductivity and Seebeck coefficient.

The calculation details of effective quality are as follows:

Step 1: Calculate the energy band and obtain the band edge position through VASPKIT 911.

Step 2: Prepare VPKIT.in as follows:

1

6

0.015

2

0.33333333 0.33333333 0.000 0.000 0.000 0.000 K- > Γ

0.33333333 0.33333333 0.000 0.500 0.000 0.000 K- > M

Step 2: Prepare VPKIT.in as follows:

Step 3: Run VASPKIT-912 or 913 to generate KPOINTS, POTCAR, and write INCAR (INCAR cannot be directly generated using VASPKIT).

Step 4: Submit the VASP task, then modify the first line of the VPKIT.in file from 1 to 2, run VASPKIT again and select 913 to obtain the following result, which is the effective mass of holes and electrons.

REFERENCES

(1) Gao, J.; Liu, Q.; Jiang, C.; Fan, D.; Zhang, M.; Liu, F.; Tang, B. The mechanical stability criterion of 7 large crystal system and its application: taking SiO_2 as an example. *Chin. J. High Press. Phys*. **2022**, 36, 051101.

(2) Bardeen, J.; Shockley, W. J. P. R. Deformation potentials and mobilities in non-polar crystals. *Phys. Rev*. **1950**, 80, 72.

(3) Xiao, Z.; Meng, W.; Wang, J.; Mitzi, D. B.; Yan, Y. Searching for promising new perovskite-based photovoltaic absorbers: the importance of electronic dimensionality. *Mater. Horiz.* **2017**, 4, 206-216.

(4) Swarnkar. A.; Marshall, A. R.; Sanehira, E. M.; Chernomordik, B. D.; Moore, D. T.; Christians, J. A.; Chakrabarti, T.; Luther, J. M. Quantum dot-induced phase stabilization of α-$CsPbI_3$ perovskite for high-efficiency photovoltaics. *Science*. **2016**, 354, 92-95.

(5) Levinshtein, M. E.; Rumyantsev, S. L.; Shur, M.; S. Properties of advanced semiconductor materials: GaN, AlN, InN, BN, SiC, SiGe. *John Wiley & Sons: U.K.* **2001**.

(6) Abd, E. H.; Ismail, Y.; Deen, M. J. A computational study of nonparabolic conduction band effect on quantum wire transport (eg GaN). *Opt. Quantum Electron*. **2013**, 45, 885-899.